Revisiting the Auto-Regressive Functions of the Cross-Entropy Ant System

Laurent Paquereau and Bjarne E. Helvik

Centre for Quantifiable Quality of Service in Communication Systems*,
Norwegian University of Science and Technology, Trondheim, Norway
{laurent.paquereau,bjarne}@q2s.ntnu.no

Abstract. The Cross-Entropy Ant System (CEAS) is an Ant Colony Optimization (ACO) system for distributed and online path management in telecommunication networks. Previous works on CEAS have enhanced the system by introducing new features. This paper takes a step back and revisits the auto-regressive functions at the core of the system. These functions are approximations of complicated transcendental functions stemming from the Cross-Entropy (CE) method for stochastic optimization, computationally intensive and therefore not suited for online and distributed operation. Using linear instead of hyperbolic approximations, new expressions are derived and shown to improve the adaptivity and robustness of the system, in particular on the occurrence of radical changes in the cost of the paths sampled by ants.

Key words: Ant-based optimization, Cross-Entropy method, CEAS, linear approximations

1 Introduction

Ant Colony Optimization (ACO) [1] systems are self-organizing systems inspired by the foraging behaviour of ants and designed to solve discrete combinatorial optimization problems. More generally, ACO systems belong to the class of Swarm Intelligence (SI) systems [2]. SI systems are formed by a population of agents, which behaviour is governed by a small set of simple rules and which, by their collective behaviour, are able to find good solutions to complex problems. ACO systems are characterized by the indirect communication between agents - (artificial) ants - referred to as stigmergy and mediated by (artificial) pheromones. In nature, pheromones are a volatile chemical substance laid by ants while walking that modifies the environment perceived by other ants. ACO systems have been applied to a wide range of problems [1]. The Cross-Entropy Ant System (CEAS) is such a system for path management in dynamic telecommunication networks.

The complexity of the problem arises from the non-stationary stochastic dynamics of telecommunication networks. A path management system should adapt

* 'Centre for Quantifiable Quality of Service in Communication Systems, Centre of Excellence" appointed by The Research Council of Norway, funded by the Research Council, NTNU, UNINETT and Telenor. http://www.q2s.ntnu.no

to changes including topological changes, e.g. link/node failures and restorations, quality changes, e.g. link capacity changes, and traffic pattern changes. The type, degree and time-granularity of changes depend on the type of network. For instance, the level of variability in link quality is expected to be higher in a wireless access network than in a wired core network.

Generally, the performance of an ACO system is related to the number of iterations required to achieve a given result. Specific to the path management problem in telecommunication networks are the additional requirements put on the system in terms of time and overhead. On changes, the system should adapt, i.e. converge to a new configuration of paths, in short time and with a small overhead. In addition, finding a good enough solution in short time is at least as important as finding the optimal solution, and there is a trade-off between quality of the solution, time and overhead.

Previous works on CEAS have improved the performance of the system by introducing new features. See for instance [3–5]. This paper follows the same objective, but takes a different approach. Rather than adding yet another mechanism, it takes a step back and revisits the auto-regressive functions at the core of the system.

The rest of this paper is organized as follows. Section 2 presents CEAS. Section 3 addresses the auto-regressive functions at the core of the system and motivates the introduction of a new set of functions. The performance of the system applying these new functions is then evaluated in Section 4. Finally, Section 5 concludes the paper.

2 Cross Entropy Ant System (CEAS)

CEAS is an online, distributed and asynchronous ACO system designed for adaptive and robust path management in telecommunication networks. Ants cooperate to collectively find and maintain minimal cost paths, or sets of paths, between source and destination pairs. Each ant performs a random search directed by the pheromone trails to find a path to a destination. Each ant also deposits pheromones so that the pheromone trails reflect the knowledge acquired by the colony thus enforcing the stigmergic behaviour characterizing ACO systems. Similarly to what happens in nature, good solutions emerge as the result of the iterative indirect interactions between ants.

Contrary to other ACO systems, the random proportional rule used by ants to decide about their next-hop and the pheromone update rule used in CEAS are formally founded and stem from the Cross-Entropy (CE) method for stochastic optimization [6]. A brief overview of these formal foundations is given below before CEAS is described in more details.

2.1 Cross-Entropy (CE) Method

The CE method is a Model-Based Search (MBS) [7] procedure applying importance sampling techniques to gradually bias a probability distribution over the

solution space (probabilistic model) towards high-quality solutions and almost surely converge to the optimal solution. An outline of the method applied to the shortest path problem is given below. For further details and proofs, the reader is referred to [6].

Let $\mathbf{G} = (\mathbf{V}, \mathbf{E})$ denote a bidirectional weighted graph where $\mathbf{V}$ is the set of vertices (nodes) and $\mathbf{E}$ the set of edges (links), and let $\mathbf{p}_t = [p_{t,vi}]_{\|\mathbf{V}\| \times \|\mathbf{V}\|}$ denote the probability distribution after t updates. Finding the shortest path between nodes s and d consists in solving the minimization problem $(\boldsymbol{\Omega}, L)$ where $\boldsymbol{\Omega}$ is the set of feasible solutions (paths) and L is the objective function, which assigns a cost $L(\boldsymbol{\omega})$ to each path $\boldsymbol{\omega} = \langle (s, v_1), (v_1, v_2), \ldots, (v_{h-1}, d) \rangle \in \boldsymbol{\Omega}$. $(v, i) \in \mathbf{E}$ denotes the link connecting node v to node i and L is an additive function, $L(\boldsymbol{\omega}) = \sum_{\forall (v,i) \in \boldsymbol{\omega}} L((v, i))$. The CE method works as follows. At each iteration t, a sample of m paths $\{\boldsymbol{\omega}_1, \ldots, \boldsymbol{\omega}_m\}$ is drawn from $\mathbf{p}_{t-1}$, and $\mathbf{p}_t$ is obtained by minimizing the cross entropy between $\mathbf{p}_{t-1}$ multiplied by a quality function Q of the cost values and $\mathbf{p}_t$, which is equivalent to solving

$$\mathbf{p}_t = \arg\max_{\mathbf{p}} \frac{1}{m} \sum_{k=1}^{m} Q(L(\boldsymbol{\omega}_k)) \sum_{(v,i) \in \boldsymbol{\omega}_k} \ln p_{vi} \ . \tag{1}$$

By choosing $Q(L(\boldsymbol{\omega}_k)) = H(L(\boldsymbol{\omega}_k), \gamma_t)$, the solution to (1) is

$$p_{t,vi} = \frac{\tau_{t,vi}}{\sum_{j \in \mathbf{N}_v} \tau_{t,vj}} \ , \tag{2}$$

where $\mathbf{N}_v = \{i \in \mathbf{V} \mid (v, i) \in \mathbf{E}\}$ and

$$\tau_{t,vi} = \sum_{k=1}^{m} I((v, i) \in \boldsymbol{\omega}_k) H(L(\boldsymbol{\omega}_k), \gamma_t) \tag{3}$$

and $I(x) = 1$ if x is true, 0 otherwise.

$$H(L(\boldsymbol{\omega}_k), \gamma_t) = e^{-\frac{L(\boldsymbol{\omega}_k)}{\gamma_t}} \tag{4}$$

is the Boltzmann function, see Fig. 1. $\gamma_t > 0$ is an internal parameter (*temperature*) determined by minimizing it subject to $h_t(\gamma_t) \geqslant \rho$, where

$$h_t(\gamma_t) = \frac{1}{m} \sum_{k=1}^{m} H(L(\boldsymbol{\omega}_k), \gamma_t) \tag{5}$$

is the overall performance function and ρ is a configuration parameter (*search focus*) close to 0, typically 0.01. Both γ_t and ρ control the relative weights given to solutions and thereby the convergence of the system. γ_t is self-adjusting and depends on the sampled solutions. ρ decides the absolute value of the temperature.

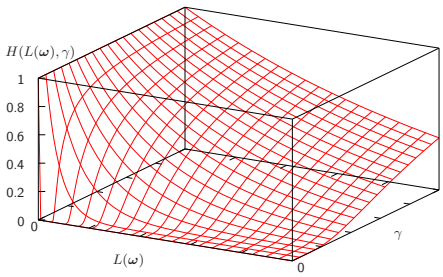

Fig. 1. Boltzmann function

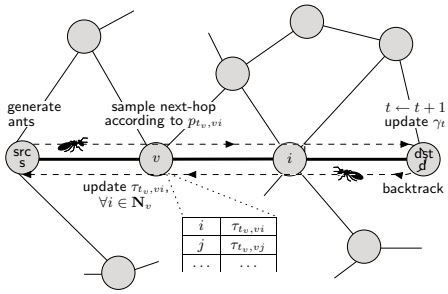

Fig. 2. Behaviour of ants in CEAS

2.2 Online Distributed Asynchronous Operation

CEAS is an implementation of the CE method as an ACO system where updates are performed online by ants at each node along their way. The CE method, as described in Section 2.1, is a centralized and batch-oriented procedure and updates are performed offline and synchronously at the end of each iteration. As such, it is therefore not suited for online, distributed and asynchronous operation. To achieve this, CEAS substitutes (3) and (5) with auto-regressive functions. Reusing the notations defined in Section 2.1, the behaviour of ants in CEAS is now detailed. See Fig. 2 for an illustration.

Starting from node s, an ant incrementally builds a path to node d by moving through a sequence of neighbour nodes. At each node, the ant samples its next-hop according to $\mathbf{p}_t$ (*biased exploration*) where t now represents the number of paths sampled. At node v, the probability that an ant decides to move to node i is given by the *random proportional rule*

$$p_{t_v,vi} = \frac{\tau_{t_v,vi}}{\sum_{j\in\mathcal{N}_v} \tau_{t_v,vj}}, \ \forall i \in \mathcal{N}_v \tag{6}$$

where $\tau_{t_v,vi}$ is the pheromone trail value at node v for the link (v,i) after t_v updates[1] at node v, see below, and $\mathcal{N}_v \subseteq \mathbf{N}_v$ is the set of neighbours of node v not yet visited by the ant. $\mathcal{N}_v = \mathbf{N}_v$ if the ant has visited none or all of the nodes in $\mathbf{N}_v$. To bootstrap the system, ants do not apply (6) but a *uniformly distributed proportional rule* (*uniform exploration*) $p_{t_v,vi} = \frac{1}{|\mathcal{N}_v|}$, $\forall i \in \mathcal{N}_v$. During normal operation, a given percentage of such *explorer ants* is maintained to allow the system to adapt to changes, e.g. to discover new solutions.

Immediately after the ant has arrived at the destination, t is incremented and the temperature γ_t is computed. The auto-regressive counterpart of (5) is

$$h_t(\gamma_t) = \beta h_{t-1}(\gamma_t) + (1-\beta) H(L(\boldsymbol{\omega}_t), \gamma_t) \ , \tag{7}$$

[1] $t_v = \sum_{x=1}^{t} I((v,\cdot) \in \boldsymbol{\omega}_x)$

which is approximated by

$$h_t(\gamma_t) \approx \frac{1-\beta}{1-\beta^t} \sum_{k=1}^{t} \beta^{t-k} H(L(\boldsymbol{\omega}_k), \gamma_t) \tag{8}$$

where $\beta \in [0,1)$ is the memory factor and $\boldsymbol{\omega}_k$ is the path sampled by the k^{th} ant arrived at the destination. γ_t is obtained by minimizing it subject to $h_t(\gamma_t) \geqslant \rho$, that is[2]

$$\gamma_t = \left\{ \gamma \mid \frac{1-\beta}{1-\beta^t} \sum_{k=1}^{t} \beta^{t-k} H(L(\boldsymbol{\omega}_k), \gamma) = \rho \right\} \ . \tag{9}$$

The ant then backtracks and updates pheromones trail values (online delayed pheromone update) along $\boldsymbol{\omega}_t$. The pheromone values are calculated according to the auto-regressive counterpart of (3)

$$\tau_{t_v,vi} = \sum_{k=1}^{t_v} I((v,i) \in \boldsymbol{\omega}_k) \beta^{t_v-k} H(L(\boldsymbol{\omega}_k), \gamma_{t_v}), \ \forall i \in \mathbf{N}_v, \ \forall v \in \boldsymbol{\pi}_t \tag{10}$$

where $\boldsymbol{\pi}_t = \langle s, v_1, v_2, \ldots, v_{h-1}, d \rangle$ denotes the sequence of nodes traversed by the ant on its way forward.

3 Auto-Regressive Functions

Both (8) and (10) are complicated transcendental functions. The exact evaluation of these functions is both processing and storage intensive. The entire path cost history $\mathbf{L}_t = \{L(\boldsymbol{\omega}_k) \mid k = 1, \ldots, t\}$ must be stored and, for each update, the weights for all the costs must be recalculated. Such requirements are impractical for the online operation of a network node. Instead, assuming that the temperature does not radically change, each term in (8) and (10) is approximated by a Taylor expansion, and these functions are replaced by a set of auto-regressive functions with limited computational and memory requirements.

Since CEAS has been first introduced in [8], $H(L(\boldsymbol{\omega}_k), \gamma)$ has been approximated using a Taylor expansion of $H(L(\boldsymbol{\omega}_k), \frac{1}{\gamma})$ around $\frac{1}{\gamma_k}$ (hyperbolic approximation). However, for a similar computational complexity, approximating $H(L(\boldsymbol{\omega}_k), \gamma)$ using a Taylor expansion around γ_k (linear approximation) provides a more accurate and more robust approximation. Details on the resulting auto-regressive schemes and their stepwise derivation are given in Appendix A.

3.1 Linear vs. Hyperbolic Approximations

Since [8], first order Taylor expansions of $H(L(\boldsymbol{\omega}_k), \frac{1}{\gamma})$, around $\frac{1}{\gamma_k}, \forall k < t$, and around γ_{t-1} for $k = t$, have been used to compute the temperature γ_t. This

[2] For $\gamma > 0$, $h_t(\gamma)$ is strictly increasing and $h_t(\gamma) \in (0,1)$. Therefore, $\forall \rho \in (0,1), \ \exists! \ \gamma_t, \ h_t(\gamma_t) = \rho$ and $\min \gamma$ s.t. $h_t(\gamma) \geqslant \rho \implies \gamma = \gamma_t$

amounts to approximating $H(L(\boldsymbol{\omega}_k), \gamma)$ by a hyperbola. Now, choosing $\rho < e^{-2}$ yields $\gamma_k < \frac{L(\boldsymbol{\omega}_k)}{2}$, unless the occurrence of a radical change in the costs of the sampled paths, see Section 3.2. Hence, $H(L(\boldsymbol{\omega}_k), \gamma)$ is convex[3] around γ_k and a linear approximation is always more accurate than a hyperbolic approximation, see Fig. 3(a). Fig. 4 shows the temperature values obtained by the exact evaluation of (9) and by applying hyperbolic and linear approximations given the same sequence of cost values. The series of costs imitates the convergence of the system. The t^{th} cost value is $L_t = L_{\min} + U_t$ where $L_{\min} = 1.0$ and U is a random variable uniformly distributed between 0 and $\frac{100}{t+1}$. The temperature values obtained using linear approximations are much closer to the exact values than the values obtained using hyperbolic approximations.

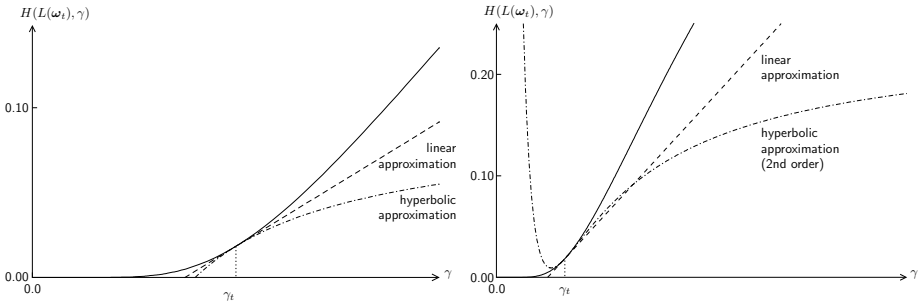

(a) Temperature calculation (b) Pheromones calculation

Fig. 3. Linear vs. hyperbolic approximations

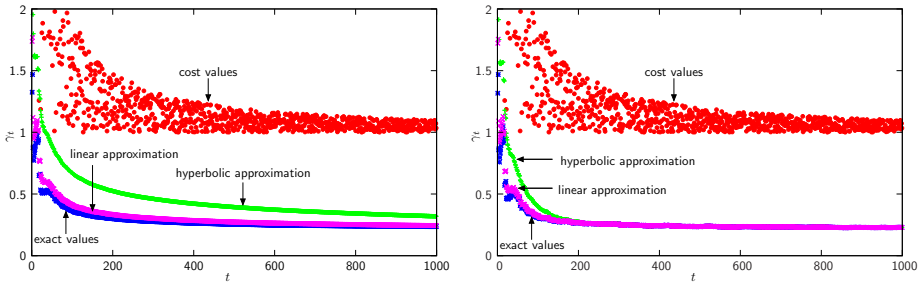

(a) $\beta = 0.998$ and $\rho = 0.01$ (b) $\beta = 0.95$ and $\rho = 0.01$

Fig. 4. Temperature obtained by numerical solution of (9) and by using hyperbolic and linear approximations

[3] $H(L(\boldsymbol{\omega}_k), \gamma)$ is convex for $\gamma \leqslant \frac{L(\boldsymbol{\omega}_k)}{2}$ and concave for $\gamma \geqslant \frac{L(\boldsymbol{\omega}_k)}{2}$.

Since [8], pheromones values are computed using second order Taylor expansions around $\frac{1}{\gamma_k}$ to avoid negative values in case of a rapid decay of the temperature. For γ close to γ_k, the second order hyperbolic expansion of $H(L(\boldsymbol{\omega}_k), \gamma_t)$ provides a better approximation than a linear approximation, see Fig. 3(b). However, when $\gamma_t < \gamma_k$ $H(L(\boldsymbol{\omega}_k), \gamma_t)$ is over-estimated[4], and when $\gamma_t > \gamma_k$ $H(L(\boldsymbol{\omega}_k), \gamma_t)$ is under-estimated. Hence, using second order expansions tends to smoothen the difference in weights given to costs as the temperature varies. As a result, it may slow down convergence as poor quality solutions (high costs) receive relatively higher weights. A first order approximation, and a fortiori a linear approximation, is therefore preferable as it provides a better approximation over a larger interval and better discriminates between good and poor solutions.

3.2 Radical Changes

This section addresses the adaptivity and robustness of the approximations to radical changes, i.e. when the assumption of small changes in the temperature does not hold anymore. Radical changes in temperature are caused by radical changes in the costs of the sampled paths, either because paths become unavailable or degraded, or because new paths are discovered. At intermediate nodes, radical temperature differences may also be observed when a node is seldom visited. For pheromone calculations, the observations made above apply, and the larger the change, the better the linear approximations compared to the hyperbolic approximations. In the following, the challenges posed by large variations in the costs of the sampled paths on the calculation of the temperature are considered. We distinguish between radically lower and radically higher costs.

Radically lower costs are observed when a radically better path is discovered. A radically better path is a path such that $L(\boldsymbol{\omega}_t) < 2\,\gamma_{t-1}$. In this case, $H(L(\boldsymbol{\omega}_t), \gamma)$ is concave around γ_{t-1}. A linear approximation may then not provide a good approximation of $H(L(\boldsymbol{\omega}_t), \gamma)$ and (9) may not have a positive solution. However, the shape of $H(L(\boldsymbol{\omega}_t), \gamma)$ can easily be exploited to provide a better approximation and ensure that a positive solution is found. See Fig. 5(a) and Appendix A for details. Using a hyperbolic approximation, (9) always have a solution, although it may be quite far from the exact value, see Fig. 5(a). It could be significantly improved by exploiting the shape of $H(L(\boldsymbol{\omega}_t), \gamma)$, but would remain less accurate than a linear approximation.

Radically higher costs are obtained for instance on the degradation of the path the system has converged to. In this case, $H(L(\boldsymbol{\omega}_t), \gamma)$ is convex around γ_{t-1}. Therefore, a linear approximation is more accurate than a hyperbolic approximation. In addition, a linear approximation is more robust than a hyperbolic approximation. The main problem with using a hyperbolic approximation is that, contrary to a linear approximation, it may be significantly smaller than $\rho, \forall \gamma > 0$. See Fig. 5(b). As a result, (9) may output a very high value or may not have a positive solution. In either case, there is no good alternative; not

[4] When $\gamma_t < \gamma_k$ and $\left|\frac{\mathrm{d}\tau_{vi,t}(\gamma)}{\mathrm{d}\gamma}\right| < 0$, the resulting over-estimation of $\tau_{vi,t}$ is only limited by $\min_{\forall \gamma} \tau_{vi,t}(\gamma)$.

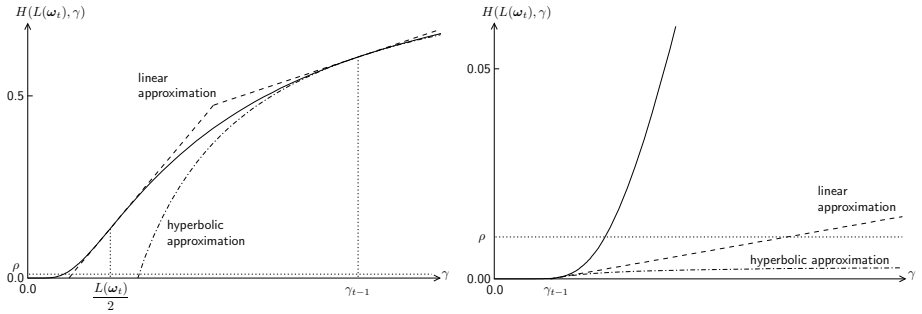

(a) Radically lower cost (b) Radically higher cost

Fig. 5. Approximation of $H(L(\boldsymbol{\omega}_t), \gamma)$ on radical changes

updating the temperature results in very low pheromone updates and therefore slow convergence, resetting the temperature in possibly premature convergence as pheromone values at intermediate nodes may be strongly directed towards a poor quality path.

The effect of radical changes in the observed costs on the approximations of the temperature is shown in Fig. 6. The settings are identical to those used for the example presented in Fig. 4, except that radical changes are introduced, namely $L_t = 0.01, \forall t \in (450, 700)$. β and ρ are chosen to illustrate the potential pitfalls described above when using hyperbolic approximations and radically higher costs are sampled, i.e. very high values (Fig. 6(a)) and no positive solution in which case γ_t is not updated (Fig. 6(b)). On the other hand, in both cases, the temperature obtained applying linear approximations correctly converges to the exact value.

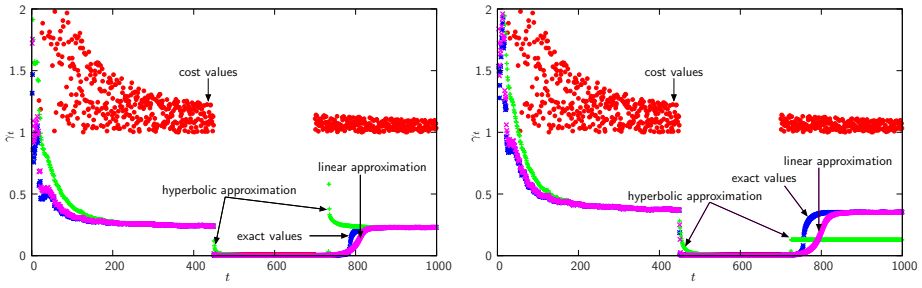

(a) $\beta = 0.95$ and $\rho = 0.01$ (b) $\beta = 0.95$ and $\rho = 0.05$

Fig. 6. Effect of radical changes on the temperature obtained by numerical solution of (9) and by using hyperbolic and linear approximations

4 Case Study

In this section, the effect of replacing the original auto-regressive update schemes obtained using hyperbolic approximations by the new schemes derived from applying linear approximations on the performance of the system is evaluated by simulation. The effect is more pronounced as good solutions are hard to find. Hence, it is demonstrated by applying CEAS to solve the `fri26` symmetric static Traveling Salesman Problem (TSP) taken from TSPLIB[5] and also used in [3]. Note that CEAS has not been specifically designed to solve the TSP. Such a hard (NP-complete) problem is chosen to stress the performance of the system.

Fig. 7 shows the mean value of the cost $L(\omega)$ of the sampled paths with respect to the number of tours completed by ants, averaged over 13 runs. Error bars indicate 95% confidence intervals. Parameter settings are similar to those used in [3] and elite selection is applied, see [3]. It is observed that applying linear approximations improves the convergence speed of the system in terms of number of iterations ("tours" here). This improvement is due to the combined effect of the faster convergence of the temperature, hence the higher relative weights given to good solutions, and the better differentiation between paths when updating pheromone levels.

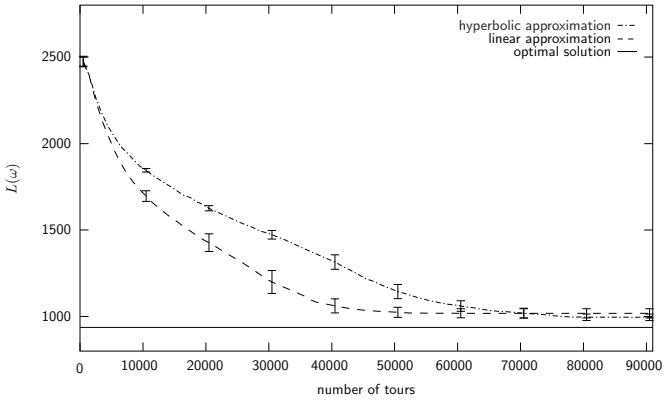

Fig. 7. 26 node TSP example

5 Conclusion

CEAS is an online, distributed and asynchronous ACO system designed for adaptive and robust path management in telecommunication networks. The performance of such a system is related to the number of iterations, the time and the

[5] `http://www.iwr.uni-heidelberg.de/groups/comopt/software/TSPLIB95`

management overhead required to converge after a change. Previous works on CEAS have improved the performance of the system by adding new mechanisms. This paper takes a step back and revisits the auto-regressive functions at the core of the system. These functions are approximations of functions stemming from the CE method for stochastic optimization, processing and storage intensive and therefore not suited for online and distributed operation. The functions used so far were based on hyperbolic approximations. In this paper, new functions are derived applying linear approximations instead. For a similar computational complexity, linear approximations are shown to be both more accurate and more robust to radical changes. Results show that the performance of the system is also improved.

References

1. Dorigo, M., Di Caro, G., Gambardella, L.M.: Ant Algorithms for Discrete Optimization. Artificial Life **5**(2) (1999) 137–172
2. Bonabeau, E., Dorigo, M., Theraulaz, G.: Swarm Intelligence: From Natural to Artificial Systems. Oxford University Press (1999)
3. Heegaard, P.E., Wittner, O.J., Nicola, V.F., Helvik, B.E.: Distributed Asynchronous Algorithm for Cross-Entropy-Based Combinatorial Optimization. In: Rare Event Simulation and Combinatorial Optimization (RESIM/COP 2004), Budapest, Hungary (2004)
4. Heegaard, P.E., Wittner, O.J.: Overhead Reduction in a Distributed Path Management System. Computer Networks, In Press. Elsevier (2009)
5. Paquereau, L., Helvik, B.E.: Ensuring Fast Adaptation in an Ant-Based Path Management System. In: 4th International Conference on Bio-Inspired Models of Network, Information, and Computing Systems (BIONETICS 2009), Avignon, France (2009)
6. Rubinstein, R.Y.: The Cross-Entropy Method for Combinatorial and Continuous Optimization. Methodology and Computing in Applied Probability (1999) 127–190
7. Zlochin, M., Birattari, M., Meuleau, N., Dorigo, M.: Model-Based Search for Combinatorial Optimization: A Critical Survey. Annals of Operations Research **131** (2004) 373–395
8. Helvik, B.E., Wittner, O.J.: Using the Cross Entropy Method to Guide/Govern Mobile Agent's Path Finding in Networks. In Goos, G., Hartmanis, J., van Leeuwen, J. (eds.): MATA 2001. LNCS, vol. 2164, pp 255–268. Springer, Heidelberg (2001)

Appendix A: Approximations Details

Temperature Calculation

Assuming that the temperature does not change radically, $H(L(\boldsymbol{\omega}_k), \gamma_t)$ is approximated by its first order Taylor expansion around γ_k for $k < t$

$$\begin{aligned} H(L(\boldsymbol{\omega}_k), \gamma_t) &\approx H(L(\boldsymbol{\omega}_k), \gamma_k) + H'(L(\boldsymbol{\omega}_k), \gamma_k)(\gamma_t - \gamma_k) \\ &= e^{-\frac{L(\boldsymbol{\omega}_k)}{\gamma_k}} + \frac{L(\boldsymbol{\omega}_k)}{\gamma_k^2} e^{-\frac{L(\boldsymbol{\omega}_k)}{\gamma_k}} (\gamma_t - \gamma_k) \\ &= e^{-\frac{L(\boldsymbol{\omega}_k)}{\gamma_k}} \left(1 - \frac{L(\boldsymbol{\omega}_k)}{\gamma_k} + \gamma_t \frac{L(\boldsymbol{\omega}_k)}{\gamma_k^2}\right) \end{aligned}$$

and $H(L(\boldsymbol{\omega}_t), \gamma_t)$ around γ_{t-1}

$$H(L(\boldsymbol{\omega}_t), \gamma_t) = e^{-\frac{L(\boldsymbol{\omega}_t)}{\gamma_t}} \approx e^{-\frac{L(\boldsymbol{\omega}_t)}{\gamma_{t-1}}} \left(1 - \frac{L(\boldsymbol{\omega}_t)}{\gamma_{t-1}} + \gamma_t \frac{L(\boldsymbol{\omega}_t)}{\gamma_{t-1}^2}\right)$$

Eq.(9) can then be rewritten

$$\begin{aligned}
\rho \frac{1-\beta^t}{1-\beta} = & \overbrace{\sum_{k=1}^{t-1} \beta^{t-k} e^{-\frac{L(\boldsymbol{\omega}_k)}{\gamma_k}} \left(1 - \frac{L(\boldsymbol{\omega}_k)}{\gamma_k}\right)}^{a_{t-1}} + \gamma_t \overbrace{\sum_{k=1}^{t-1} \beta^{t-k} e^{-\frac{L(\boldsymbol{\omega}_k)}{\gamma_k}} \frac{L(\boldsymbol{\omega}_k)}{\gamma_k^2}}^{b_{t-1}} \\
& + e^{-\frac{L(\boldsymbol{\omega}_t)}{\gamma_{t-1}}} \left(1 - \frac{L(\boldsymbol{\omega}_t)}{\gamma_{t-1}} + \gamma_t \frac{L(\boldsymbol{\omega}_t)}{\gamma_{t-1}^2}\right) \\
= & \, a_{t-1} + e^{-\frac{L(\boldsymbol{\omega}_t)}{\gamma_{t-1}}} \left(1 - \frac{L(\boldsymbol{\omega}_t)}{\gamma_{t-1}}\right) + \gamma_t \left(b_{t-1} + \frac{L(\boldsymbol{\omega}_t)}{\gamma_{t-1}^2} e^{-\frac{L(\boldsymbol{\omega}_t)}{\gamma_{t-1}}}\right)
\end{aligned}$$

Hence, γ_t is obtained as

$$\gamma_t = -\frac{a_{t-1} + e^{-\frac{L(\boldsymbol{\omega}_t)}{\gamma_{t-1}}} \left(1 - \frac{L(\boldsymbol{\omega}_t)}{\gamma_{t-1}}\right) - \rho \frac{1-\beta^t}{1-\beta}}{b_{t-1} + \frac{L(\boldsymbol{\omega}_t)}{\gamma_{t-1}^2} e^{-\frac{L(\boldsymbol{\omega}_t)}{\gamma_{t-1}}}}$$

where a_t and b_t can be expressed as auto-regressive functions:

$$\begin{aligned}
a_t &\leftarrow \beta \left(a_{t-1} + e^{-\frac{L(\boldsymbol{\omega}_t)}{\gamma_t}} \left(1 - \frac{L(\boldsymbol{\omega}_t)}{\gamma_t}\right)\right) \\
b_t &\leftarrow \beta \left(b_{t-1} + e^{-\frac{L(\boldsymbol{\omega}_t)}{\gamma_t}} \frac{L(\boldsymbol{\omega}_t)}{\gamma_t^2}\right)
\end{aligned}$$

and the initial values are $a_0 = b_0 = 0$ and $\gamma_0 = -\frac{L(\boldsymbol{\omega}_1)}{\ln \rho}$.

Now when $\gamma_{t-1} > \frac{L(\boldsymbol{\omega}_t)}{2}$ [6], the first order Taylor expansion around γ_{t-1} may not be a good approximation of $H(L(\boldsymbol{\omega}_t), \gamma_t)$ and may even result in a negative value for γ_t. A better approximation may be obtained by approximating $H(L(\boldsymbol{\omega}_t), \gamma_t)$ by its tangent at the inflection point $(\frac{L(\boldsymbol{\omega}_t)}{2}, e^{-2})$. The value obtained using this approximation is used as a lower bound for γ_t when $\rho < e^{-2}$ and $\gamma_{t-1} > \frac{L(\boldsymbol{\omega}_t)}{2}$. See Fig. 8 for an illustration. Hence, if $\gamma_{t-1} > \frac{L(\boldsymbol{\omega}_t)}{2}$, γ_t is calculated as

$$\gamma_t = \max\left(-\frac{a_{t-1} - e^{-2} - \rho \frac{1-\beta^t}{1-\beta}}{b_{t-1} + \frac{4}{L(\boldsymbol{\omega}_t)} e^{-2}}, -\frac{a_{t-1} + e^{-\frac{L(\boldsymbol{\omega}_t)}{\gamma_{t-1}}} \left(1 - \frac{L(\boldsymbol{\omega}_t)}{\gamma_{t-1}}\right) - \rho \frac{1-\beta^t}{1-\beta}}{b_{t-1} + \frac{L(\boldsymbol{\omega}_t)}{\gamma_{t-1}^2} e^{-\frac{L(\boldsymbol{\omega}_t)}{\gamma_{t-1}}}}\right)$$

[6] This happens when a radically better path is discovered.

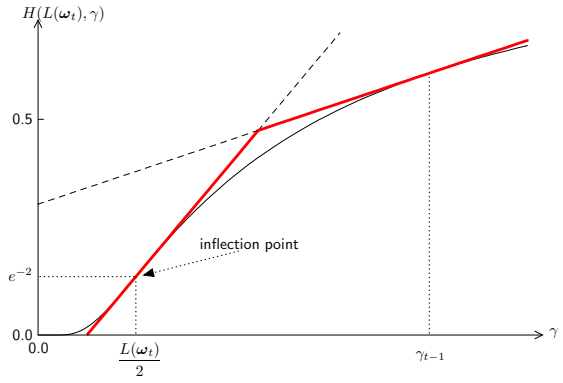

Fig. 8. Approximation of $H(L(\boldsymbol{\omega}_t), \gamma_t)$ for $\gamma_{t-1} > \frac{L(\boldsymbol{\omega}_t)}{2}$

Pheromones Calculation

Eq.(10) can be rewritten

$$\tau_{t_v,vi} = I((v,i) \in \boldsymbol{\omega}_{t_v}) H(L(\boldsymbol{\omega}_{t_v}), \gamma_{t_v}) + \underbrace{\sum_{k=1}^{t_v-1} I((v,i) \in \boldsymbol{\omega}_k) \beta^{t_v-k} H(L(\boldsymbol{\omega}_k), \gamma_{t_v})}_{\tau_{t_v,vi}|_{(v,i) \notin \boldsymbol{\omega}_{t_v}}}$$

Approximating $\tau_{t_v,vi}|_{(v,i) \notin \boldsymbol{\omega}_t}$ by a weighted sum of first order Taylor expansions gives

$$\tau_{t_v,vi}|_{(v,i) \notin \boldsymbol{\omega}_{t_v}} \approx \overbrace{\sum_{k=1}^{t_v-1} I((v,i) \in \boldsymbol{\omega}_k) \beta^{t_v-k} e^{-\frac{L(\boldsymbol{\omega}_k)}{\gamma_k}} \left(1 - \frac{L(\boldsymbol{\omega}_k)}{\gamma_k}\right)}^{A_{t_v-1,vi}}$$
$$+ \gamma_{t_v} \overbrace{\sum_{k=1}^{t_v-1} I((v,i) \in \boldsymbol{\omega}_k) \beta^{t_v-k} e^{-\frac{L(\boldsymbol{\omega}_k)}{\gamma_k}} \frac{L(\boldsymbol{\omega}_k)}{\gamma_k^2}}^{B_{t_v-1,vi}}$$

where $A_{t_v,vi}$ and $B_{t_v,vi}$ can be expressed as auto-regressive functions:

$$A_{t_v,vi} \leftarrow \beta \left(A_{t_v-1,vi} + I((v,i) \in \boldsymbol{\omega}_{t_v}) e^{-\frac{L(\boldsymbol{\omega}_{t_v})}{\gamma_{t_v}}} \left(1 - \frac{L(\boldsymbol{\omega}_{t_v})}{\gamma_{t_v}}\right)\right)$$

$$B_{t_v,vi} \leftarrow \beta \left(B_{t_v-1,vi} + I((v,i) \in \boldsymbol{\omega}_{t_v}) e^{-\frac{L(\boldsymbol{\omega}_{t_v})}{\gamma_{t_v}}} \frac{L(\boldsymbol{\omega}_{t_v})}{\gamma_{t_v}^2}\right)$$

and where the initial values are $A_{0,vi} = B_{0,vi} = 0$. In addition, $\tau_{t_v,vi}|_{(v,i) \notin \boldsymbol{\omega}_{t_v}}$ is bounded by 0 and $\sum_{k=1}^{t-1} \beta^{t-k} = \beta \frac{1-\beta^{t-1}}{1-\beta}$.